Translocation and cleavage of myocardial dystrophin as a common pathway to advanced heart failure: A scheme for the progression of cardiac dysfunction

Teruhiko Toyo-Oka*†‡§, Tomie Kawada¶, Jumi Nakata*, Han Xie*, Masashi Urabe‖, Fujiko Masui*, Takashi Ebisawa*, Asaki Tezuka*, Kuniaki Iwasawa†‡, Toshiaki Nakajima‡, Yoshio Uehara†, Hiroyuki Kumagai**, Sawa Kostin††, Jutta Schaper††, Mikio Nakazawa‡‡, and Keiya Ozawa‖

*Department of Pathophysiology and Internal Medicine, †Health Service Center, and ‡Department of Cardiovascular Medicine, University of Tokyo, Tokyo 113-0033, Japan; ¶Division of Pharmacy and ‡‡Department of Medical Technology, Niigata University, Niigata 951-8520, Japan; ‖Division of Gene Therapy, Jichi Medical School, Tochigi 329-0498, Japan; **Department of Pharmacology, Gunma University, Maebashi 371-8511, Japan; and ††Department of Experimental Cardiology, Max Planck Institute, Bad Nauheim 61231, Germany

Communicated by Setsuro Ebashi, Okazaki National Research Institutes, Okazaki, Japan, March 25, 2004 (received for review January 24, 2004)

Advanced heart failure (HF) is the leading cause of death in developed countries. The mechanism underlying the progression of cardiac dysfunction needs to be clarified to establish approaches to prevention or treatment. Here, using TO-2 hamsters with hereditary dilated cardiomyopathy, we show age-dependent cleavage and translocation of myocardial dystrophin (Dys) from the sarcolemma (SL) to the myoplasm, increased SL permeability *in situ*, and a close relationship between the loss of Dys and hemodynamic indices. In addition, we observed a surprising correlation between the amount of Dys and the survival rate. Dys disruption is not an epiphenomenon but directly precedes progression to advanced HF, because long-lasting transfer of the missing *δ-SG* gene to degrading cardiomyocytes *in vivo* with biologically nontoxic recombinant adenoassociated virus (rAAV) vector ameliorated all of the pathological features and changed the disease prognosis. Furthermore, acute HF after isoproterenol toxicity and chronic HF after coronary ligation in rats both time-dependently cause Dys disruption in the degrading myocardium. Dys cleavage was also detected in human hearts from patients with dilated cardiomyopathy of unidentified etiology, supporting a scheme consisting of SL instability, Dys cleavage, and translocation of Dys from the SL to the myoplasm, irrespective of an acute or chronic disease course and a hereditary or acquired origin. Hereditary HF may be curable with gene therapy, once the responsible gene is identified and precisely corrected.

Despite the steady progress of pharmaceutical therapy, it is still difficult to completely prevent heart failure (HF) from proceeding to an advanced stage. Cardiac transplantation is the last choice to save the patient at the end stage, and this treatment entails many sociomedical problems. An alternative strategy for therapy is urgently required (1, 2). Primary or secondary degradation of dystrophin (Dys) might be of great significance in determining the cause of HF. Muscular dystrophy results in HF, and poor outcome in patients and animal models is associated with genetic mutations of Dys or the sarcoglycan (SG) complex (1–6). In the present study, we examined the following phenomena: (*i*) the time course of the hemodynamics with biventricular catheterization under stable anesthesia (7) until the TO-2 animals started to show overt HF and cardiac death; (*ii*) *in situ* sarcolemma (SL) stability by double fluoromicroscopy for the entry of an SL-impermeable dye, Evans blue dye (EB), into cardiomyocytes (8) and immunostaining of Dys or δ-SG; (*iii*) Western blotting of Dys and protein quantification; (*iv*) the correlation between limited proteolysis of Dys and hemodynamics; and (*v*) *in vivo* gene transduction in TO-2 hamsters. We also evaluated pathological features in rats with acute and acquired HF due to isoproterenol (Isp) toxicity (9) and in humans with advanced dilated cardiomyopathy (DCM).

Materials and Methods

Experimental Animals, the *rAAV* Vector Gene Construct, and *in Vivo* Gene Delivery. Male F_1B (control) and TO-2 hamster strains were obtained from Bio Breeders (Watertown, MA), and rAAV/lacZ vector alone or a mixture of recombinant adenoassociated virus (rAAV)/lacZ and rAAV/δ-SG was intramurally injected into the cardiac apex of the 5-week-old hamsters (7). pW1, an rAAV plasmid containing lacZ or a 1.2-kb fragment of δ-SG cDNA flanked by inverted terminal repeats of the AAV genome, pHLP19, a helper plasmid with *rep* and *cap* genes, and pladeno-1, a plasmid harboring the adenovirus *E2A*, *E4*, and *VA* genes, were used for rAAV/lacZ or rAAV/δ-SG production. pWSG with a δ-SG expression cassette driven by a cytomegalovirus (CMV) promoter was used for rAAV/δ-SG production (7, 8). Under open chest surgery with constant-volume ventilation, rAAV/lacZ alone or a mixture of rAAV/lacZ and rAAV/δ-SG was intramurally injected into the cardiac apex twice (each injection was 15 μl, for a total of 8.4×10^{10} and 6×10^{10} copies for lacZ and δ-SG, respectively).

Morphological and Immunological Analyses. A polyclonal, site-directed antibody to δ-SG was prepared at a high titer, by using a synthetic peptide with a sequence deduced from the cloned cDNA as a specific epitope (4). Monoclonal antibodies to Dys and to the transgene of lacZ (β-galactosidase) were obtained from NovoCastra (Newcastle, U.K.) and Funakoshi (Tokyo). The density of antibody-specific bands for the rod domain of Dys was measured within a linear intensity range for the applied amount of protein, after Western blotting of whole-heart homogenates, by 5–15% SDS/PAGE. For the Isp study, 10–20% SDS/PAGE was used to detect degradation products of both Dys and δ-SG. To simultaneously monitor Dys disruption, SL fragility *in situ*, and expression of the δ-SG transgene, double fluoromicroscopy was used to detect immunostaining of Dys with a FITC-labeled antibody specific to the rod domain of Dys, the entry of membrane-impermeable EB into cardiomyocytes, and immunostaining of δ-SG with a rhodium isothiocyanate (RITC)-labeled specific antibody by using a Nikon Diaphot or a Leica (Heidelberg, Germany) TCS SL confocal microscope. Where indicated, the Dys immunoproduct in the SL and myoplasm was semiquantified on cardiomyocytes, with or without transduction of δ-SG in the same observation field.

Abbreviations: HF, heart failure; Dys, dystrophin; SG, sarcoglycan; SL, sarcolemma; EB, Evans blue dye; Isp, isoproterenol; DCM, dilated cardiomyopathy; rAAV, recombinant adenoassociated virus; LVP, left ventricular pressure; EDP, end diastolic pressure; CVP, central venous pressure.

§To whom correspondence should be addressed. E-mail: toyooka_3im@hotmail.com.

Table 1. Cardiac hemodynamics with progression of HF

Strain	Age, weeks	LVP, mmHg	dP/dt_{max}, mmHg/sec	dP/dt_{min}, mmHg/sec	EDP, mmHg	CVP, mmHg
F_1B	5	82.9 ± 1.2	4,385 ± 91	−4,503 ± 208	3.1 ± 0.6	1.70 ± 0.53
	15	132.9 ± 5.5†	8,188 ± 743†	−7,188 ± 971†	1.8 ± 1.5	0.78 ± 0.50
	25	132.5 ± 6.9	6,709 ± 188	−6,513 ± 602	1.7 ± 2.7	0.46 ± 0.21
	40	125.1 ± 9.6	7,063 ± 290	−7,180 ± 576	1.6 ± 0.9	−0.62 ± 0.32
TO-2	5	83.0 ± 2.1	4,599 ± 192	−5,175 ± 233*	1.9 ± 0.3*	2.82 ± 0.17*
	15	100.2 ± 4.7*†	4,645 ± 637*	−3,664 ± 378*†	8.8 ± 1.9*†	2.70 ± 0.87*
	25	87.9 ± 8.3*	5,240 ± 388*	−3,171 ± 80*	12.8 ± 1.6*	3.12 ± 0.88*
	40	80.0 ± 2.8*	4,283 ± 97*	−3,120 ± 145*	18.0 ± 1.4*†	9.35 ± 1.35*†

Hemodynamic indices measured under stable anesthesia (7, 8): LVP, its maximum derivative (dP/dt_{max}) and minimum derivative (dP/dt_{min}), EDP, and CVP, in control (F_1B strain) and hereditary DCM (TO-2 strain) hamsters. Each value is shown as the mean ± SE (n = 4–8 hamsters in each group). * and † indicate statistical significance ($P < 0.05$) compared with the F_1B strain and the preceding age, respectively.

Hemodynamic Studies and Statistical Analyses. Peak left ventricular pressure (LVP), left ventricular end diastolic pressure (EDP), its first derivative (dP/dt), and central venous pressure (CVP) were measured under stable anesthesia (7, 8). All values were expressed as the mean ± SE and evaluated by paired Student's t test, ANOVA, and correlation analyses. A P value of <0.05 was considered significant.

Results and Discussion

Progression of DCM to Advanced HF in TO-2 Hamsters. Control F_1B hamsters showed growth-dependent increases in the peak LVP, the maximum rate of LVP (dP/dt_{max}), and the minimum rate of LVP (dP/dt_{min}, Table 1). In contrast, TO-2 hamsters persistently demonstrated systolic failure characterized by reduced LVP, dP/dt_{max}, and blunted dP/dt_{min}. Congestive HF was documented by increased left ventricular EDP and CVP. These signs became aggravated between 25 and 40 weeks of age, when the rate of cardiac death sharply increased (see below). The EDP and CVP reached levels 9.5 and 3.3 times higher, respectively, than those at 5 weeks of age.

Translocation of Dys from the SL to the Myoplasm During DCM Progression. Cardiac samples from TO-2 hamsters revealed time-dependent pathological features at each age (Fig. 1). After 5 weeks, double fluoromicroscopy showed that Dys was neatly arranged on the SL, and EB administered *i.v.* before killing the animals did not enter the myoplasm, indicating that the integrity of the SL was well preserved. After 25 and 40 weeks, the Dys on the SL became blurred, and some cardiomyocytes demonstrated a shift of Dys from the SL to the myoplasm. We refer to this phenomenon as "translocation" of Dys. These cardiomyocytes matched exactly with cells that took up EB (within ovals), denoting that the SL of the translocated cells leaked the exogenously applied dye.

Cleavage of Dys in Hamster Heart and in the Hearts of Humans with DCM. Western blotting of the myocardial homogenate with an antibody specific to the rod domain of Dys showed characteristic features (Fig. 2*a Left*). Normal hearts at 5 weeks of age showed a band at 430 kDa corresponding to normal Dys, and the staining intensity was preserved up to 40 weeks of age. Striking differences were observed in TO-2 hamsters, although at 5 and 15 weeks of age the staining pattern did not differ from that of the F_1B heart. However, at 25 weeks of age, extra bands were detected between 60 and 200 kDa (Fig. 2*a Left*), and the intensity of the Dys 430-kDa band started to decline. The intensity of this band was markedly reduced between 25 and 40 weeks of age, whereas the intensity of the 60-kDa band increased, mirroring the Dys band (Fig. 2*b*). The period of significant Dys cleavage matched exactly the periods when Dys translocation became

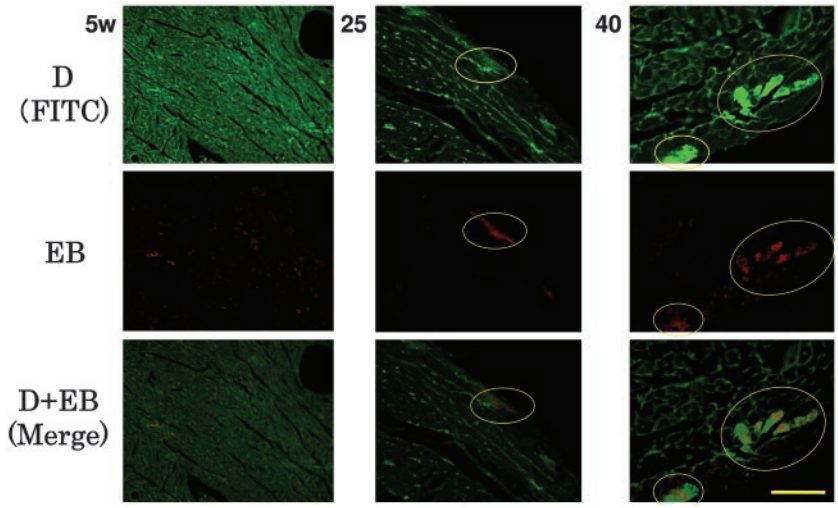

Fig. 1. Age-dependent translocation of Dys and increased permeability of the SL during HF progression in TO-2 hamsters. Double fluoromicroscopy for detection of a FITC-labeled antibody to the rod domain of Dys and entry of membrane-impermeable, fluorescent EB, at 5, 25, and 40 weeks of age (w). Cardiomyocytes demonstrating a shift of Dys from the SL to the myoplasm are shown in ovals. (Bar = 40 μm.)

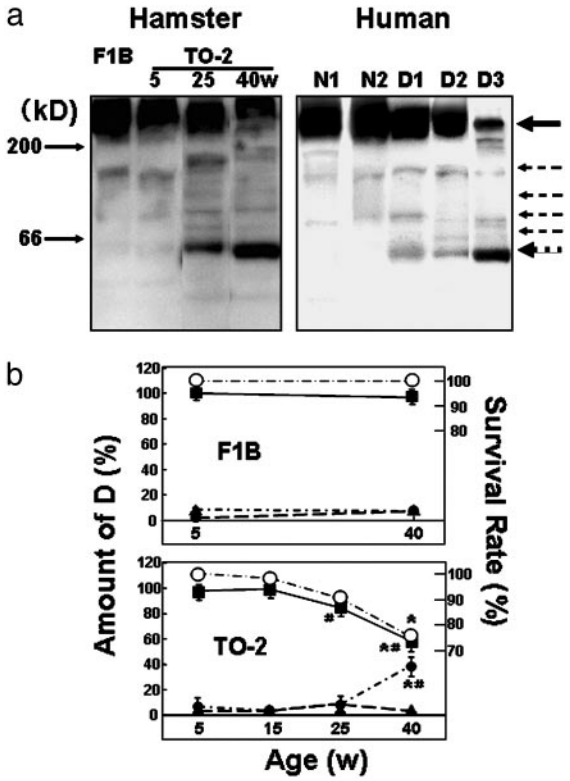

Fig. 2. Cleavage and reduction of cardiac Dys during DCM progression in hamsters and humans. (*a Left*) Control (F_1B strain) or DCM (TO-2 strain) hamsters at 5, 25, and 40 weeks of age (w). (*a Right*) Normal human myocardium (N1 and N2) and DCM hearts (D1, D2, and D3) at the time of cardiac transplantation. A solid arrow at 430 kDa and several dotted arrows denote the original Dys and its degradation products, respectively, after 5–20% SDS/PAGE of whole-heart homogenates. (*b*) Time course of the survival rate of control (F_1B; *Upper*) or DCM (TO-2; *Lower*) hamsters (○) and the density of immunoreactive bands specific to the rod domain of Dys at 430 (■), 60 (●) or 160 (▲) kDa. * and # indicate a significant difference, compared with the control F_1B strain and the preceding age, respectively.

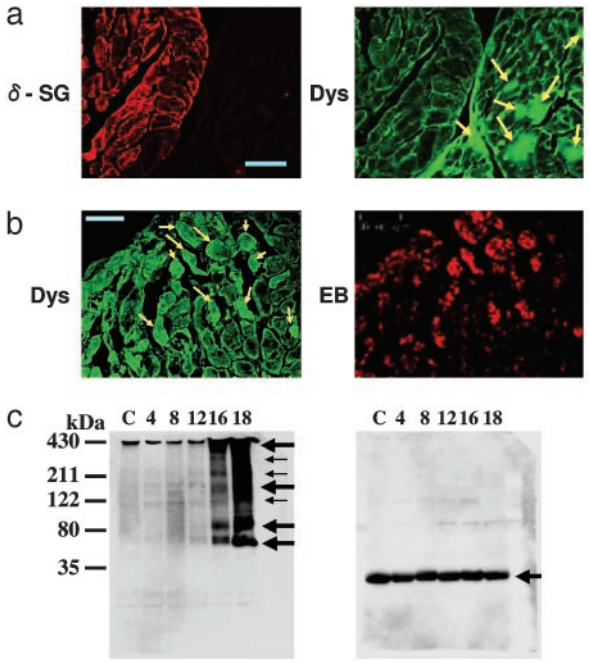

Fig. 3. (*a*) Double immunostaining of δ-SG (rhodamine isothiocyanate) and Dys (FITC) of TO-2 hamster hearts 35 weeks after local δ-*SG* gene transfection *in vivo* (8). Arrows indicate cardiomyocytes where dystrophin was translocated from the SL to the myoplasm. (Bar = 40 μm.) (*b*) Assessment of Dys translocation (FITC) and SL fragility *in situ* (EB entry) 16 h after the administration of Isp at a high dose (10 mg/kg i.p.) in Wistar rats (15). Arrows indicate cardiomyocytes where dystrophin was translocated from the SL to the myoplasm. (Bar = 40 μm.) (*c*) Western blotting of Dys (*Left*) and δ-SG (*Right*) from the same rat heart homogenate sample after gradient 10–15% SDS/PAGE of the control (C) and 4, 8, 12, 16 and 18 h after Isp treatment. Arrows indicate uncleaved Dys (430 kDa) and Dys degradation products (*Left*) or δ-SG (*Right*).

evident (Fig. 1) and when the animals started to die of congestive HF (ref. 8 and Fig. 2*b*). The intensity of the faint 160-kDa band did not change throughout the study and appeared to be unrelated to the progression of HF.

Similar cleavage of Dys was confirmed in hearts from patients with DCM of unidentified etiology who had undergone cardiac transplantation (Fig. 2*a Right*). The topological shift of Dys was also documented in samples of advanced stage DCM (unpublished data). Accordingly, the translocation was common to both animal models and patients with DCM. Other antibodies to the C or N terminus of Dys did not clearly recognize the cleavage product (data not shown). At present, we do not know the reason for this discrepancy in human cases of advanced HF showing selective cleavage of Dys at the N terminus (10).

Relationship of Dys Cleavage to Hemodynamics and the Lifespan of Hamsters. Surprisingly, the amount of Dys or its 60-kDa-band degradation product in TO-2 animals very closely correlated with the hemodynamic indices that characterize the progression of HF. The Dys amount was positively correlated with the systolic index [peak LVP, coefficient of regression (r) = 0.998 and $P < 0.0004$], and negatively correlated with the diastolic parameters (EDP, $r = 0.996$ and $P < 0.0005$; CVP, $r = 0.954$ and $P < 0.002$). The intensity of the 60-kDa band showed a clear negative correlation with the LVP ($r = 0.961$, $P < 0.002$) and a positive correlation with the EDP ($r = 0.954$, $P < 0.002$) and CVP ($r = 0.996$, $P < 0.0005$). These highly significant regression coefficients for correlation of the amount of Dys with systolic or diastolic performance support a tentative role for Dys in transmitting an effect through the actin–myosin linkage to the extracellular matrix. It is also noteworthy that no correlation was found between the amounts of Dys or the 60-kDa band and the dP/dt_{max} or dP/dt_{min} value (data not shown), both of which are regulated by Ca^{2+} handling (11) and the energetics of cardiac muscle cells (12). It should be emphasized that a distinct relationship was found between the amount of Dys or the 60-kDa band and the survival rate of the TO-2 animals over time (Fig. 2*b Lower*). It is possible that these immunological and hemodynamic data could be biased, because ≈30% of the TO-2 hamsters died of HF (Fig. 2*b Lower*), and we could only use the survivors in the analysis.

Effect of Long-Lasting Gene Therapy on Dys Localization. The final evidence that the disruption of Dys is not an epiphenomenon in HF but is actually caused by a loss of δ-SG is provided by the double immunostaining of Dys and δ-SG in TO-2 hearts with or without local gene transfection *in vivo* (Fig. 3*a*). In control F_1B hearts, both proteins were equally expressed on the SL (data not shown). In contrast, the TO-2 heart did not express δ-SG (13). As described above (Fig. 1), Dys staining became blurred with age, and some cardiomyocytes revealed Dys translocation (14). Gene delivery of normal δ-SG *in vivo*, by means of a nonpathogenic and long-lasting rAAV vector (7, 8), was used to locally express the δ-SG transgene, and this gene therapy completely ameliorated Dys translocation in the same cardiomyocytes for up to 35 weeks (Fig. 3*a Left*). In contrast, nontransfected cells

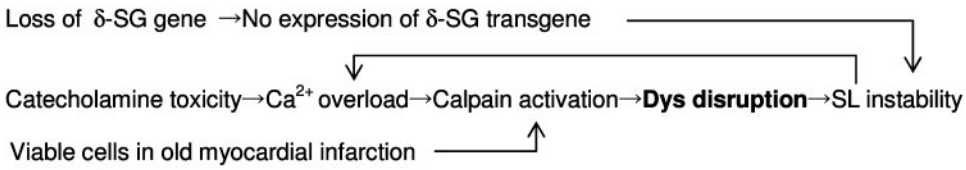

Scheme 1. Pathways for the progression of HF to an advanced stage.

showed translocation of Dys in the same sample (indicated by arrows in Fig. 3*a Right*). This finding specifically eliminates the possibility that Dys disruption resulted from the parallel development of HF, because Dys translocation was restricted to cardiomyocytes that did not express the δ-SG transgene. Furthermore, the amount of Dys estimated *in situ* by densitometry of immunofluoromicroscopic images in cardiomyocytes indicated a 1.22 ± 0.13 fold ($P < 0.01$) preferential localization of Dys on the SL of δ-SG-transfected cells ($n = 70$ cells per group).

Effect of Isp on SL Permeability, and Shift and Cleavage of Dys and δ-SG. A toxic dose of Isp (10 mg/kg i.p.) causes acute HF and morphological deterioration in normal rats (9). Pathological examination has shown time-dependent degradation of Dys and apoptosis of cardiomyocytes from 4 to 18 h after Isp was administered (15). Confocal microscopy of cardiomyocytes in the same observation field showed translocation of Dys (indicated by arrows in Fig. 3*b Left*) and entry of the SL-impermeable EB into the myoplasm of cardiac muscle cells. The shift of Dys was selectively detected 16 h after Isp treatment only in cardiomyocytes where EB had entered the myoplasm (Fig. 3*b Right*). Western blotting revealed time-dependent cleavage of Dys, showing degradation fragments between 60 and 200 kDa (Fig. 3*c Left*). In contrast, δ-SG was not hydrolyzed at all (Fig. 3*c Right*). Immunohistology confirmed that δ-SG did not shift from the SL but remained localized on the SL (data not shown). The effect of high-dose Isp, a β-adrenergic agonist, was similar to that observed in a DCM mouse with a protein kinase A knock-in gene (16). To verify the therapeutic effect of gene therapy in a β-adrenergic agonist/protein kinase A/phospholamban system, the pharmacological action (17, 18) and the disease prognosis need to be precisely examined, because an improvement in hemodynamics does not always prolong the lifespan of the animal (19).

The limited hydrolysis of Dys, common to the models of acute and chronic diseases in the present study, suggests a role for calpain, because cardiomyocytes contain an appreciable amount of this protein (20), and intracellular Ca^{2+} handling is modified in failing hearts (21, 22). Neither a specific inhibitor for calpain nor a calpain knockout animal is currently available to test this hypothesis. β-Adrenergic agonists induce Ca^{2+} overload in cardiomyocytes by increasing Ca^{2+} uptake (23). In addition, Dys and α-, β-, and γ-SG, but not δ-SG, are hydrolyzed by the endogenous protease (24) or isolated calpain *in vitro* (25, 26). The preferential breakdown of these proteins, but not δ-SG, in three HF models, i.e., TO-2 hamster hearts (13), Isp-treated rat hearts (Fig. 3*b*), and viable cells at the end stage of myocardial infarction (26), might be accompanied by substantially enhanced activity of *m*-calpain over its endogenous inhibitor, calpastatin. The expression of *m*-calpain in TO-2 hearts markedly exceeded that of calpastatin during the progression of HF (data not shown). These results may imply that the balance between calpain and calpastatin will shift in a calpain-dominant manner. Furthermore, dot hybridization analyses revealed no increment of mRNA of each DAP component under these HF conditions, suggesting that compensatory biosynthesis did not occur in the case of DAP.

A Scheme for the Progression of HF to an Advanced Stage. The clinical link between excess stimulation with catecholamines and myocardial damage has been confirmed by the therapeutic success of β-adrenergic antagonists in TO-2 hamsters (27) and humans (28, 29). The cleavage of Dys has also been documented after enterovirus infection, resulting in DCM-like HF (30). These pathological findings present a paradigm in which cardioselective cleavage of Dys may lead to progression of HF to an advanced stage (Scheme 1). Scheme 1 does not exclude the involvement of a protease cascade, as seen through the activation of a calpain-like homologue in neuronal degeneration in *Caenorhabditis elegans* (31), or involvement of the ubiquitin/proteasome system (32) in the loss of Dys. More definite evidence is required to precisely determine the causative factor(s). This common pathological process, irrespective of the hereditary or acquired origin and the chronic or acute course of the disease, suggests a strategy for the treatment of advanced HF through interruption of the vicious circle by either gene therapy or drug treatment.

We thank Dr. John R. Solaro (Department of Physiology and Biophysics, University of Illinois, Chicago) for discussion of the results and Dr. Y. Niwa and K. Kurosawa (Department of Pathophysiology, University of Tokyo) for experimental and secretarial assistance. This work was supported by Ministry of Education, Culture, and Science Grant A2 142070333 and by the Ministry of Welfare and Labor, Japan, the Mitsubishi Research Foundation, and the Motor Vehicle Foundation.

1. Cox, G. F. & Kunkel, L. M. (1997) *Curr. Opin. Cardiol.* **12,** 329–343.
2. Seidman, J. G. & Seidman, C. (2001) *Cell* **104,** 557–567.
3. Durbeej, M. & Campbell, K. P. (2002) *Curr. Opin. Genet. Dev.* **12,** 349–361.
4. Sakamoto, A., Ono, K., Abe, M., Jasmin, G., Eki, T., Murakami, Y., Masaki, T., Toyo-oka, T. & Hanaoka, F. (1997) *Proc. Natl. Acad. Sci. USA* **94**, 13873–13878.
5. Nigro, V., Okazaki, Y., Belsito, A., Piluso, G., Matsuda, Y., Politano, L., Nigro, G., Ventura, C., Abbondanza, C., Molinari, A. M., *et al.* (1997) *Hum. Mol. Genet.* **6**, 601–607.
6. Tsubata, S., Bowles, K. R., Vatta, M., Zintz, C., Titus, J., Muhonen, L., Bowles, N. E. & Towbin, J. A. (2000) *J. Clin. Invest.* **106,** 655–662.
7. Kawada, T., Sakamoto, A., Nakazawa, M., Urabe, M., Masuda, F., Hemmi, C., Wang, Y., Shin, W. S., Nakatsuru, Y., Sato, H., *et al.* (2001) *Biochem. Biophys. Res. Commun.* **284**, 431–435.
8. Kawada, T., Nakazawa, M., Nakauchi, S., Yamazaki, K., Shimamoto, R., Urabe, M., Nakata, J., Masui, F., Nakajima, T., Suzuki, J., *et al.* (2002) *Proc. Natl. Acad. Sci. USA* **99**, 901–906.
9. Kahn, D. S., Rona, G. & Chappel, C. I. (1969) *Ann. N.Y. Acad. Sci.* **156,** 285–293.
10. Vatta, M., Stetson, S. J., Perez-Verdia, A., Entman, M. L., Noon, G. P., Torre-Amione, G., Bowles, N. E. & Towbin, J. A. (2002) *Lancet* **359,** 936–941.
11. Ebashi, S., Nonomura, Y., Toyo-oka, T. & Katayama, E. (1976) *Symp. Soc. Exp. Biol.* **30**, 349–360.
12. Toyo-oka, T., Nagayama, K., Suzuki, J. & Sugimoto, T. (1992) *Circulation* **86,** 295–301.
13. Kawada, T., Nakatsuru, Y., Sakamoto, A., Koizumi, T., Shin, W. S., Okai-Matsuo, Y., Suzuki, J., Uehara, Y., Nakazawa, M., Satoh, H., *et al.* (1999) *FEBS Lett.* **458,** 405–408.
14. Kawada, T., Hemmi, C., Fukuda, S., Iwasawa, K., Tezuka, A., Nakazawa, M., Sato, H. & Toyo-oka, T. (2004) *Exp. Clin. Cardiol.* **8,** in press.
15. Xi, H., Shin, W. S., Suzuki, J., Nakajima, T., Kawada, T., Uehara, Y., Nakazawa, M. & Toyo-oka, T. (2000) *J. Cardiovasc. Pharmacol.* **36,** Suppl. 2, S25–S29.
16. Antos, C. L., Frey, N., Marx, S. O., Reiken, S., Gaburjakova, M., Richardson, J. A., Marks, A. R. & Olson, E. N. (2001) *Circ. Res.* **89,** 997–1004.

17. Bristow, M. R. (2001) *Circulation* **103,** 787–788.
18. Hoshijima, M., Ikeda, Y., Iwanaga, Y., Minamisawa, S., Date, M. O., Gu, Y., Iwatate, M., Li, M., Wang, L., Wilson, J. M., *et al.* (2002) *Nat. Med.* **8,** 864–871.
19. Jessup, M. & Brozena, S. (2003) *N. Engl. J. Med.* **348,** 2007–2018.
20. Toyo-oka, T., Shimizu, T. & Masaki, T. (1978) *Biochem. Biophys. Res. Commun.* **82,** 484–491.
21. Gwathmey, J. K., Copelas, L., MacKinnon, R., Schoen, F. J., Feldman, M. D., Grossman, W. & Morgan, J. P. (1987) *Circ. Res.* **61,** 70–76.
22. Whitmer, J. T., Kumar, P. & Solaro, R. J. (1988) *Circ. Res.* **62,** 81–85.
23. Naylor, W. G., Mas-Oliva, J. & Williams, A. J. (1980) *Circ. Res.* **46,** Part 2, 161–166.
24. Koenig, M. & Kunkel, L. M. (1990) *J. Biol. Chem.* **265,** 4560–4566.
25. Yoshida, M., Suzuki, A., Shimizu, T. & Ozawa, E. (1992) *J. Biochem.* **112,** 433–439.
26. Yoshida, H., Takahashi, M., Koshimizu, M., Tanonaka, K., Oikawa, R., Toyo-oka, T. & Takeo, S. (2003) *Cardiovasc. Res.* **59**, 419–427.
27. Opie, L. H., Walpoth, B. & Barsacchi, R. (1985) *J. Mol. Cell. Cardiol.* **17,** Suppl. 2, 21–34.
28. Gottlieb, S. S., McCarter, R. J. & Vogel, R. A. (1998) *N. Engl. J. Med.* **339,** 489–497.
29. Packer, M., Coats, A. J., Fowler, M. B., Katus, H. A., Krum, H., Mohacsi, P., Rouleau, J. L., Tendera, M., Castaigne, A., Roecker, E. B., *et al.* (2001) *N. Engl. J. Med.* **344,** 1651–1658.
30. Badorff, C., Lee, G. H., Lamphear, B. J., Martone, M. E., Campbell, K. P., Rhoads, R. E. & Knowlton, K. U. (1999) *Nat. Med.* **5,** 320–326.
31. Syntichaki, P., Xu, K., Driscoll, M. & Tavernarakis, N. (2002) *Nature* **419,** 939–944.
32. Bonuccelli, G., Sotgia, F., Schubert, W., Park, D. S., Frank, P. G., Woodman, S. E., Insabato, L., Cammer, M., Minetti, C. & Lisanti, M. P. (2003) *Am. J. Pathol.* **163,** 1663–1675.